



Large insulating gap in topological insulators induced by negative spin-orbit splitting

Julien Vidal,¹ Xiuwen Zhang,² Vladan Stevanović,¹ Jun-Wei Luo,¹ and Alex Zunger^{3,*}

¹National Renewable Energy Laboratory, Golden, Colorado 80401, USA

²Department of Physics, Colorado School of Mines, Golden, Colorado 80401, USA

³University of Colorado, Boulder, Colorado 80309, USA

(Received 7 February 2012; revised manuscript received 16 May 2012; published 24 August 2012)

In a cubic topological insulator (TI), there is a band inversion whereby the s -like Γ_{6c} conduction band is below the p -like $\Gamma_{7v} + \Gamma_{8v}$ valence bands by the “inversion energy” $\Delta_i < 0$. In TIs based on the zinc-blende structure such as HgTe, the Fermi energy intersects the degenerate Γ_{8v} state so the insulating gap E_g between occupied and unoccupied bands vanishes. To achieve an insulating gap $E_g > 0$ critical for TI applications, one often needs to resort to structural manipulations such as structural symmetry lowering (e.g., Bi_2Se_3), strain, or quantum confinement. However, these methods have thus far opened an insulating gap of only < 0.1 eV. Here we point out that there is an electronic rather than structural way to affect an insulating gap in a TI: if one can invert the spin-orbit levels and place Γ_{8v} below Γ_{7v} (“negative spin-orbit splitting”), one can realize band inversion ($\Delta_i < 0$) with a large insulating gap (E_g up to 0.5 eV). We outline design principles to create negative spin-orbit splitting: hybridization of d orbitals into p -like states. This general principle is illustrated in the “filled tetrahedral structures” (FTS) demonstrating via GW and density functional theory (DFT) calculations $E_g > 0$ with $\Delta_i < 0$, albeit in a metastable form of FTS.

DOI: [10.1103/PhysRevB.86.075316](https://doi.org/10.1103/PhysRevB.86.075316)

PACS number(s): 73.43.-f, 31.15.A-, 72.25.Hg, 73.20.-r

I. INTRODUCTION

In conventional cubic insulators such as GaAs or CdTe [Fig. 1(a)] the s -like conduction band $\Gamma_{6c}^{(2)}$ lies above the p -like valence band $\Gamma_{8v}^{(4)} + \Gamma_{7v}^{(2)}$, thus defining a positive “inversion energy” $\Delta_i = E[\Gamma_{6c}^{(2)}] - \max(E[\Gamma_{8v}^{(4)}], E[\Gamma_{7v}^{(2)}])$ (superscript denotes degeneracy). It has been known for a long time¹ that as the elements making up common cubic insulators become progressively heavier, e.g., in the sequence $\text{ZnTe} \rightarrow \text{CdTe} \rightarrow \text{HgTe}$ or $\text{Si} \rightarrow \text{Ge} \rightarrow \text{Sn}$, the s -like $\Gamma_{6c}^{(2)}$ moves down in energy (a relativistic Mass-Darwin effect²) and eventually (e.g., HgTe or α -Sn) dive below p -like $\Gamma_{8v}^{(4)}$ leading to $\Delta_i < 0$, i.e., band inversion. Recently^{3,4} it was pointed out that when such band inversion occurs at time-reversal invariant wave vectors it produces interesting electronic properties, e.g., Dirac cones inside the insulating bulk band gap. The observation^{3,5} and usefulness of such effects necessitate that in addition to a negative inversion energy $\Delta_i < 0$ there must be a positive “insulating gap” E_g ; i.e., the lowest-unoccupied states lie above the highest occupied state. Small band-gap TIs, on the other hand, lead to two obstacles to realize TI-based devices at room temperature. First, the omnipresent carrier-producing defects have a significant effect in small gap materials as they impede the tuning of the Fermi level.⁶ Second, in narrow gap materials, the generally present band bending has a particularly large effect on narrowing the gap.⁷

In a normal insulator such as CdTe [Fig. 1(a)], the positive inversion energy Δ_i equals the insulating gap E_g [Fig. 1(a)], but in a cubic TI such as HgTe [Fig. 1(c)] $\Delta_i < 0$ is associated with $E_g = 0$. As is evident from Fig. 1(c), this results from the fact that the $\Gamma_{6c}^{(2)}$ state which dives below the $\Gamma_{8v}^{(4)}$ state is twofold degenerate (including spin) whereas, in HgTe, $\Gamma_{8v}^{(4)}$ state is fourfold degenerate (including spin), so the Fermi level dissects $\Gamma_{8v}^{(4)}$ and results in $E_g = 0$. The opening of an insulating band gap can be accomplished in conventional materials by

splitting the degeneracy of the Γ_{8v} -like state via application of external nonuniform strain (as was proposed in LuPtBi⁸) or by selecting noncubic materials with sufficiently low symmetry to create a natural (“crystal-field”) splitting (e.g., chalcopyrite⁹ or in rhombohedral Bi_2Se_3) or by quantum confinement pushing the highest occupied state down and the lowest unoccupied state up.^{10,11} However, finding materials with band inversion ($\Delta_i < 0$) yet with large positive insulating gap E_g has not been easy with conventional TI materials. To date, many of them displayed semimetallic or very small insulating gap $E_g < 0.1$ eV, with very few materials such as Bi_2Se_3 being above 0.2 eV.

In this paper we suggest an *electronic* mechanism to create a significant insulating gap (larger than 0.5 eV in some cases), yet with band inversion. It is based on the observation that the order of $\Gamma_{7v}^{(2)}$ and $\Gamma_{8v}^{(4)}$ in cubic materials can be switched between “ Γ_{8v} -above- Γ_{7v} ” [“positive spin-orbit (SO) splitting” $\Delta_{so} > 0$, Figs. 1(a) and 1(c)] and “ Γ_{8v} -below- Γ_{7v} ” [“negative spin-orbit splitting” $\Delta_{so} < 0$, Figs. 1(b) and 1(d)]. In the latter case, if in addition Δ_i is significantly negative then there is a natural insulating gap between the unoccupied $\Gamma_{7v}^{(2)}$ and the occupied $\Gamma_{8v}^{(4)}$. We show that $\Delta_{so} < 0$ can be designed by increasing d character (not the usual p character) in $\Gamma_{7v}^{(2)} + \Gamma_{8v}^{(4)}$, and we point to a group of materials likely to have this property. The existence of a topological Mott insulator for some negative spin-orbit systems^{12–15} has been recently proposed. In these cases, an insulating gap would result from a complex interplay between electron-electron correlation, spin-orbit coupling, and crystal-field splitting.¹⁶ Thus, a mechanism based purely on negative spin orbit has yet to find a stable candidate material. Nevertheless, we propose specific design principles which might help in identifying TI systems having large insulating gaps without the use of nanostructuring or application of external nonuniform strain.

II. POSITIVE VERSUS NEGATIVE EFFECTIVE SPIN-ORBIT SPLITTING

The spin-orbit splitting in cubic binary materials is given by $\Delta_{\text{so}} = E(\Gamma_{8v}) - E(\Gamma_{7v})$. Negative spin-orbit splitting was experimentally observed for the first time in the case of ZnO in the 1960s^{17,18} and shortly after was explained by Shindo *et al.*¹⁹ and Cardona:²⁰ within a cubic lattice, spin-orbit interaction gives d orbitals a negative splitting between $j = 3/2$ and $1/2$ states, whereas to p orbitals it gives a positive splitting. The following expression has been proposed to express spin-orbit splitting of materials as a function of the contribution from p - and d -orbital atomic spin-orbit splitting:

$$\Delta_{\text{so}} = A[\alpha_p \Delta_{\text{so}}^{(p)} - \alpha_d \Delta_{\text{so}}^{(d)}], \quad (1)$$

where α_p (α_d) is the p (d) character at $\Gamma_{8v}^{(4)} + \Gamma_{7v}^{(2)}$, $\Delta_{\text{so}}^{(p)}$ ($\Delta_{\text{so}}^{(d)}$) are the atomic spin-orbit splittings of p (d) states, and A is a renormalization factor. In CdTe [Fig. 1(a)] and HgTe [Fig. 1(c)], $\Gamma_{7v} + \Gamma_{8v}$ (Γ_{4v} without spin-orbit coupling) is strongly Te- p and the metal d state is rather far from $\Gamma_{7v} + \Gamma_{8v}$ so its mixing is small and α_d is nearly zero, thus $\Delta_{\text{so}} > 0$. In CuCl, on the other hand, the Cu- d orbitals are close to $\Gamma_{7v} + \Gamma_{8v}$ and hybridize strongly, so α_d is large and $\Delta_{\text{so}} < 0$. Unfortunately, CuCl is not a TI, i.e., $\Delta_i > 0$.²⁰ However, much stronger negative spin-orbit splitting has been reported, most notably for Cu-based materials such as copper halide.²⁰ Large negative spin-orbit splitting comparable to the one of p states in Sb, Te, or Bi has been reported in the case of d states such as in Os, Ir, Pt, or Au.^{21,22} Equation (1) illustrates that the need for inversion $\Delta_i < 0$ with $\Delta_{\text{so}} < 0$ might be counterindicated, as $\Delta_i < 0$ often requires heavy anion elements, yet minimizing $\Delta_{\text{so}}^{(p)}$ implies light anion elements. The resolution will be described below.

III. METHODS

The stability of each compound has been assessed through the use of total-energy calculation based on GGA + U,²³ as implemented in the Vienna *ab initio* simulation package. The reciprocal space is sampled using grids with densities of

$2\pi \times 0.068$ and $2\pi \times 0.051 \text{ \AA}^{-1}$ for relaxation and static calculation, respectively. For total-energy calculation, we use U parameters $U = 3 \text{ eV}$ on the d orbital. For Lu, we use $U = 9 \text{ eV}$ on the f orbital. In addition to the stability of each crystal structure, we have also investigated the thermodynamical stability of each compound with respect to dissociation into elements or binary compounds following the procedure prescribed in Ref. 23. The determination of the topological order has been carried out at the GW level as described in a previous publication.²⁴ Spin-orbit splitting was calculated self-consistently within density-functional theory²⁵ and added as a first-order perturbation to the GW results.

IV. STABILITY OF THE INVESTIGATED MATERIALS

In the following sections, we present either existing or hypothetical materials which display both negative spin-orbit splitting and nontrivial topological order. More precisely, the group of filled tetrahedral structures (FTS) (Y/La/Lu)-(Pd/Pt)-(Sb/Bi) is thermodynamically stable and referenced numerous times in the FTS crystal structures (see Refs. 26–29 and enclosed references). On the other hand, we find that within the group of compounds (Li,Na,K,Rb)-(Au)-(O,S) and (Sc,Y,La,Lu)-(Au)-C neither of the FTS modifications are the ground-state structures, involving other crystal-structure types instead. Finally, we investigate the thermodynamical stability of kesterite $\text{Au}_2\text{HgPbS}_4$ and conclude that $\text{Au}_2\text{HgPbS}_4$ is thermodynamically unstable with respect to decomposition into Au_2S , HgS , and PbS_2 .

V. CRYSTAL STRUCTURES AND NATURE OF VALENCE-BAND MAXIMUM OF FTS

In order to seek materials with $\Delta_i < 0$ (heavy elements having large Mass-Darwin relativistic lowering of the conduction s -like Γ_{6c}) yet $\Delta_{\text{so}} < 0$ one needs large d character in the otherwise p -like $\Gamma_{8v} + \Gamma_{7v}$. To accomplish this, we leave the binary systems and move to ternaries. Binary zinc blende with cation at $T_1 = (0,0,0)$ and anion at $T_2 = (\frac{1}{4}, \frac{1}{4}, \frac{1}{4})$ has significant empty space between the atoms (only 64–66%

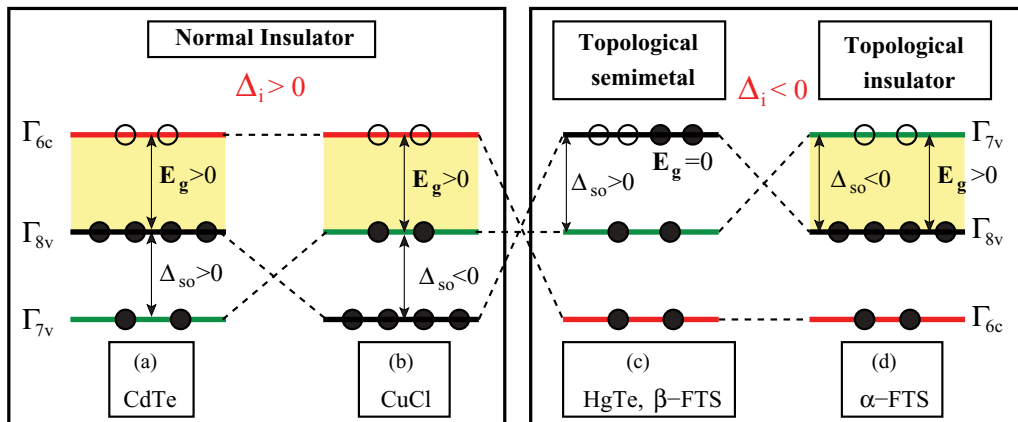


FIG. 1. (Color online) Definition of normal insulator, topological semimetal, and topological insulator for tetrahedral structures. Solid dots represent electrons while open dots represent holes. Δ_{so} refers to the spin-orbit splitting at Γ while Δ_i refers to the inversion energy. Yellow shading corresponds to the insulating band gap E_g .

of the unit cell volume is occupied if touching spheres are assumed). If either of the two empty interstitial sites $IT_1 = (\frac{1}{2}, \frac{1}{2}, \frac{1}{2})$ or $IT_2 = (\frac{3}{4}, \frac{3}{4}, \frac{3}{4})$ are occupied, we create “filled tetrahedral structures.”³⁰⁻³³ In α -type FTS, the IT_1 position is occupied by a “stuffing atom” and IT_2 is empty, whereas in β -type FTS the IT_2 position is occupied by a “stuffing atom” and IT_1 is empty. We will designate α -FTS by the atoms sequence occupying IT_1 - T_1 - T_2 and β -FTS by the atoms sequence occupying IT_2 - T_1 - T_2 . The β structure can be derived from the α -FTS by exchanging the sites of the atoms located at T_1 and T_2 .

VI. GROUP OF $IT_{1,2}$ - T_1 - $T_2 = (Y/La/Lu)$ -(Pd/Pt)-(Sb/Bi) FTS

In this group of materials we expect that $\Gamma_{8v}^{(4)} + \Gamma_{7v}^{(2)}$ will have a considerable transition-metal d character which would potentially lead to negative SO splitting. Figure 2(a) presents the calculated Δ_{so} of α -FTS (red diamond and gray shading) and β -FTS (black circles and Bordeaux shading), indeed showing $\Delta_{so} < 0$ that is composition and structure dependent. The explanation of the trends in Δ_{so} observed in Fig. 2(a) requires a closer look into the electronic structure of the valence-band maximum (VBM) in these systems as well as the differences between the α and β phases, and we will use a specific compound LuPtBi as a showcase while conclusions remain valid for other members of this group. Namely, as already discussed by Gruhn,³⁴ bonding in FTS is accompanied by a charge transfer between the least electronegative Lu and mostly covalently bonded (PtBi) group. Bi- p orbitals and both p and d orbitals of the transition metals participate in the bonding since the tetrahedral symmetry of both FTS structures allows for the onsite p - d mixing on the transition-metal site. As can be seen from Fig. 2(b) it is the interplay between Lu- d and Pt- p and $-d$ orbitals at the VBM that explains the much more negative Δ_{so} in the α phase than in the β phase. In the case of α -FTS, it is the contributions of Pt- d orbitals to the electronic states at the VBM that govern to a large

extent the magnitude of the spin-orbit splitting at Γ . Indeed, Bi is coordinated by four Pt and four Lu atoms. Therefore, due to electrostatic reasons, the charge transferred from Lu “prefers” to be localized mostly on Bi atoms which then appear as anions. On the other hand, in β -FTS, Bi and Pt exchange their roles: Pt is now the first neighbor to both Lu and Bi and takes the anion role. Therefore, a larger portion of Pt electronic shells got filled and then both d and p characters originating from Pt atoms appear at the VBM. On the other hand, for α -FTS, only the d shell got filled. A similar argument could be applied to Lu except that the d shell of Lu is completely empty and therefore p states from Lu never mix to the VBM. Trends in Δ_{so} observed in Fig. 2(a) simply follow trends in $\Delta_{so}^{(d)}$ and $\Delta_{so}^{(p)}$ across the periodic table. Total-energy stability calculations of the stable crystal structures have, thus far, shown that the structural modification with $\Delta_i < 0$ and $\Delta_{so} < 0$ (α -FTS) is less stable (by 0.4 eV/atom) than the structural modification [β -FTS, Fig. 1(c)] with $\Delta_i < 0$ but $\Delta_{so} > 0$. This can be understood following Gruhn’s argument that the β phase is the most stable phase when the most electronegative atom plays the role of the anion.³⁴

This analysis is supported by our SO calculation depicted in Fig. 2, where we show the calculated spin-orbit splitting of α (red) and β (black) structures of a series of FTS compounds $(IT)-(T_1)-(T_2)$ with elements (Y,La,Lu) -(Pd,Pt)-(Sb,Bi), respectively. To correlate the resulting Δ_{so} of Fig. 2(a) with the orbital character, we show in Figs. 2(b) and 2(c) the orbital character of $\Gamma_{8v}^{(4)} + \Gamma_{7v}^{(2)}$ in these two structural modifications, showing the above-noted differences between the VBM character in the α - and β -FTS. The degree of $\Delta_{so} < 0$ depends not only on the existence of a large contribution of d character at $\Gamma_{8v}^{(4)} + \Gamma_{7v}^{(2)}$ but also on having extended d orbitals, i.e., contributing significantly to the spin-orbit splitting as demonstrated in Fig. 2. It is evident from the abrupt change in spin-orbit splitting for the β -type FTS while going from Y to (La,Lu) [see Fig. 2(a)] that $4d$ elements of Y,Pd contribute marginally to Δ_{so} while $5d$ elements of La,Lu,Pt make Δ_{so} negative. Within this family of materials, we find LuPtBi in the assumed α structure to be TI with a large excitation gap of 0.52 eV along with a negative inversion energy $\Delta_i = -1.0$ eV.

VII. DESIGN PRINCIPLES

The study of the (Y,La,Lu) -(Pd,Pt)-(Sb,Bi) family together with the previous knowledge on HgTe allows us to propose some design principles for large excitation gap TI. Band inversion $\Delta_i < 0$ induced by large Z scalar relativistic effects can be implemented by considering either heavy anions (such as $X = Te$ in HgX instead of $X = S$) or heavy cations (such as $M = Tl$ in CuMS₂ instead of $M = In$). To get $\Delta_{so} < 0$, we search for materials with VBM with $\alpha_d \Delta_{so}^{(d)}$ as large as possible compared to $\alpha_p \Delta_{so}^{(p)}$. This implies choosing light anion (minimize $\Delta_{so}^{(p)}$) and late $5d$ row elements as cations (maximize $\Delta_{so}^{(d)}$). The presence of extended $5d$ states at $\Gamma_{8v}^{(4)} + \Gamma_{7v}^{(2)}$ is beneficial to $\Delta_i < 0$ since $6s$ states are more likely to invert with $(5p,5d)$ states. On the other hand, the presence of p states from a light anion at VBM is required for obtaining the parity inversion with the conduction-band minimum (CBM) and without contributing much to

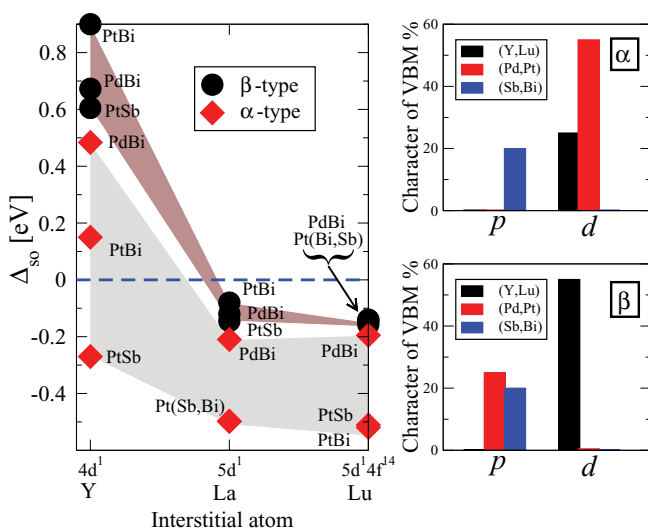


FIG. 2. (Color online) Left panel: spin-orbit splitting (in eV) for FTS with different interstitial atom in α - and β -type structures. Right panel: p and d contribution to the character of the valence-band maximum for the α -type FTS (top) and β -type FTS (bottom).

spin-orbit splitting. The main disadvantages of d orbitals for $\Delta_{so} < 0$ is the small absolute value of their atomic spin-orbit splitting relative to p orbitals with the same principal quantum number.³⁵ Because of the light anion, this might not appear as an obvious concern. Yet, another pitfall of $5d$ orbitals is the possible intra-atomic mixing in the VBM of $6p$ -like states coming from low-lying unoccupied orbitals of the $5d$ elements.³⁶ Such onsite mixing can be prevented though by the adequate choice of local symmetry, which forbids mixing of p states and d states such as O_h , or by placing it next to more electronegative atoms and thereby enforcing the cation role, such as in the case of α -LuPtBi. This design principle suggests that materials involving elements such as Pt ($\Delta_{so}^{5d} \approx 1.5$ eV²¹), Ir ($\Delta_{so}^{5d} \approx 1.3$ eV²¹), Os ($\Delta_{so}^{5d} \approx 1.06$ eV²¹), or Re ($\Delta_{so}^{5d} \approx 0.85$ eV²¹) should be considered when searching for new topological insulators. Overall, the Au element occupies a sweet spot in the periodic table: besides a large atomic spin-orbit splitting of 1.5 eV,²¹ it has a full $5d$ shell which lies high in energy and therefore is more likely to form the VBM. Furthermore, Au has a rather deep $6s$ orbital, which could favor band inversion $\Delta_i < 0$. We next explore two Au-based cases.

VIII. GROUP OF $IT_{1,2}-T_1-T_2 = (Li,Na,K,Rb)-(Au)-(O,S)$ AND $IT_{1,2}-T_1-T_2 = (Sc,Y,La,Lu)-(Au)-C$ FTS³⁷

According to our self-consistent GW (scGW) calculation, most of these materials have a negative inversion energy in the α -FTS except for KAUS and RbAuS (see Fig. 3). The (Y,La,Lu)AuC family shows the same character of the VBM as in the previously described (Y,Lu,La)(Pd,Pt)(Sb,Bi) family, i.e., mixing of d states from Au (40%) and (Sc,Y,La,Lu) (20%) with p states from C (40%). On the other hand, (Li,Na,K,Rb)-(Au)-(O,S) displays a more conventional p - d character originating from the anion (O,S) (50%) and Au (50%). Li, Na, K, and Rb do not participate directly in the character of the VBM, yet they induce volume change which affects the character of the VBM and the renormalization factor

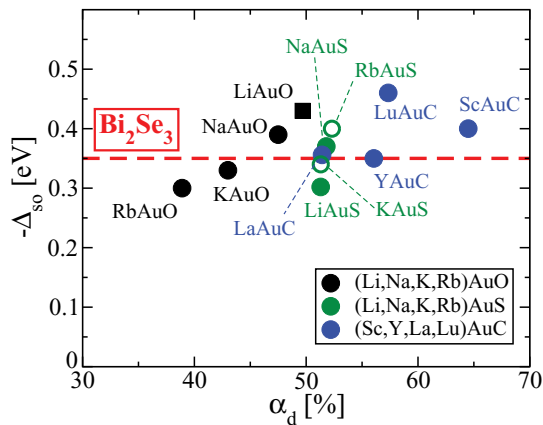


FIG. 3. (Color online) Spin-orbit splitting at Γ vs the d character of the VBM at Γ for different FTS. All FTS are in α type. The broken red line displays the value of the excitation gap for Bi_2Se_3 . Hollow symbols refer to trivial semiconductors and metals, squares refer to indirect band gap, and circles refer to direct band gap; i.e., the band gap is fully defined by the spin-orbit splitting $\Delta_{so} = E_g$.

A of Eq. (1). Figure 3 displays their spin-orbit splitting at Γ for the group (Li,Na,K,Rb)-(Au)-(O,S) and (Sc,Y,La,Lu)-(Au)-C. One should first notice that the VBM might occur slightly away from Γ and consequently induces indirectness of the excitation gap such as for LiAuO.³⁸ Then, the spin-orbit induced excitation gap is further reduced by the energy difference between the VBM and last occupied state at Γ . In the case of LiAuO, the excitation gap is reduced by ≈ 0.12 eV with respect to the spin-orbit splitting at Γ . On the other hand, the CBM is fully determined by the spin-orbit splitting at Γ . *Without negative spin-orbit splitting at Γ , all of these compounds would have been topological metals.* The band inversion occurring at Γ is likely to induce a metallic behavior. An s -like conduction band near Γ in β -LuPtBi gets occupied, which explains the experimental observation in β -type LuPtBi.³⁹ When searching for new topological insulators, one should take special care in localizing the true VBM by means of GW-based methods. Most of the materials presented in Fig. 3 have excitation gaps comparable to the largest band gap reported experimentally for a topological insulator, namely, Bi_2Se_3 . However, even though the α -type structure is more stable than the β -type structure for the (Li,Na,K,Rb)Au(O,S) and the (Sc,Y,Lu,La)AuC families, we find that neither of the FTS modifications are the ground state involving other structure types instead.

IX. KESTERITE STRUCTURE OF Au_2HgPbS_4

Cu- and Ag-based kesterite materials have been proposed to be topological insulators, together with a mechanism opening excitation gap.⁴⁰ Kesterite structure could be viewed as a zincblende A_4X_4 lattice where the cation site A could be occupied by three different atoms $a_2 + b + c$ instead of one. Such symmetry lowering $A_4 \rightarrow a_2 + b + c$ results in a distortion of the crystal structure and subsequently in the crystal-field splitting of $\Gamma_{8v}^{(4)}$ and $\Gamma_{7v}^{(2)}$. It was proposed that tuning of the crystal-field splitting through lattice distortions could open a large excitation gap of about 30 meV in the kesterite family, the best of class being $Ag_2HgPbSe_4$ with a band gap of 54 meV.⁴⁰ We consider instead the Au-analog kesterite Au_2HgPbS_4 as it follows some of the design principles previously stated: increase of $5d$ character at the VBM, choice of a light anion S, and prevention of the $6p$ orbitals of Pb from mixing to the VBM through enforcement of its oxidation state to +IV. Our scGW calculation shows that Au_2HgPbS_4 presents an inverted band gap, making it a topologically nontrivial material. Furthermore, in Au_2HgPbS_4 , the splitting of $\Gamma_{8v}^{(4)}$ and $\Gamma_{7v}^{(2)}$ due to the crystal field is marginal (≈ 10 meV⁴¹) while spin-orbit splitting at Γ is rather large, $\Delta_{so} = 0.26$ eV. However, Au_2HgPbS_4 presents a metallic character due to a low-lying occupied conduction band at high-symmetry point $(\frac{1}{2}, \frac{1}{2}, 0)$ producing a small electron pocket at this \mathbf{k} point. Nevertheless, the case of Au_2HgPbS_4 is noteworthy as it shines light on the potential magnitude of a spin-orbit induced excitation gap with respect to a strain-induced excitation gap, the latter being one of the most popular methods for an excitation gap opening in the field of topological insulators. The spin-orbit induced excitation gap originates only from atomic properties (i.e., type of orbitals) and does not depend much on the crystal structure (at least at the level of first-order

perturbation) as it is the case for crystal-field splitting or strain. Therefore, such an excitation gap must be much more robust with respect to crystal deformation than strain-induced gap.

X. CONCLUSIONS

In conclusion, we present design principles for large excitation gap topological insulators based on negative spin-orbit coupling. Based on our *ab initio* calculations, we prove that the presence of extended *d* orbitals could induce a large excitation gap and also favors topological order. Possible drawbacks were discussed and possible work-arounds were introduced. The potential of our design principle was tested on two groups of materials in FTS structures and $\text{Au}_2\text{HgPbS}_4$ in kesterite structure. However, most of these materials are proven not thermodynamically stable in the FTS structure or unstable with respect to decomposition into binaries. Therefore, a search effort involving *5d* elements and

a light anion should be pursued, with the reward of finding large excitation gap TIs.

ACKNOWLEDGMENTS

We thank S. Lany for fruitful discussions. Research was supported by the US Department of Energy, Office of Basic Sciences, Division of Materials Sciences and Engineering, under Contract No. DE-AC36-08GO28308 to National Renewable Energy Laboratory (NREL). X. Z. acknowledges support by the US Department of Energy, Office of Science, Basic Energy Sciences, Energy Frontier Research Centers, under Contract No. DE-AC36-08GO28308 to NREL. X. Z. also acknowledges the administrative support of Renewable Energy Materials Research Science and Engineering at the Colorado School of Mines, Golden, Colorado. The use of massively parallel processing capabilities at the National Energy Research Scientific Computing Center is gratefully acknowledged.

*alex.zunger@colorado.edu

- ¹L. I. Berger, *Semiconductor Materials* (CRC, Boca Raton, 1997).
- ²B. Thaller, *The Dirac Equation* (Springer-Verlag, New York, 1992).
- ³M. Z. Hasan and C. L. Kane, *Rev. Mod. Phys.* **82**, 3045 (2010).
- ⁴J. Moore, *Nature (London)* **464**, 194 (2010).
- ⁵X. L. Qi and S. C. Zhang, *Rev. Mod. Phys.* **83**, 1057 (2011).
- ⁶Z. Ren, A. A. Taskin, S. Sasaki, K. Segawa, and Y. Ando, *Phys. Rev. B* **82**, 241306 (2010).
- ⁷J. G. Checkelsky, Y. S. Hor, R. J. Cava, and N. P. Ong, *Phys. Rev. Lett.* **106**, 196801 (2011).
- ⁸W. Al-Sawai, H. Lin, R. S. Markiewicz, L. A. Wray, Y. Xia, S.-Y. Xu, M. Z. Hasan, and A. Bansil, *Phys. Rev. B* **82**, 125208 (2010).
- ⁹W. Feng, D. Xiao, J. Ding, and Y. Yao, *Phys. Rev. Lett.* **106**, 016402 (2011).
- ¹⁰B. A. Bernevig, T. L. Hughes, and S.-C. Zhang, *Science* **314**, 1757 (2006).
- ¹¹J.-W. Luo and A. Zunger, *Phys. Rev. Lett.* **105**, 176805 (2010).
- ¹²D. Pesin and L. Balents, *Nature Physics* **6**, 376 (2010).
- ¹³H.-M. Guo and M. Franz, *Phys. Rev. Lett.* **103**, 206805 (2009).
- ¹⁴X. Wan, A. M. Turner, A. Vishwanath, and S. Y. Savrasov, *Phys. Rev. B* **83**, 205101 (2011).
- ¹⁵H.-C. Jiang, Z.-C. Gu, X.-L. Qi, and S. Trebst, *Phys. Rev. B* **83**, 245104 (2011).
- ¹⁶C. Martins, Ph.D. thesis, Ecole Polytechnique, 2010.
- ¹⁷D. Thomas, *J. Phys. Chem. Solids* **15**, 86 (1960).
- ¹⁸J. Hopfeld, *J. Phys. Chem. Solids* **15**, 97 (1960).
- ¹⁹K. Shindo, A. Morita, and H. Kamimura, *J. Phys. Soc. Jpn.* **20**, 2054 (1965).
- ²⁰M. Cardona, *Phys. Rev.* **129**, 69 (1963).
- ²¹J. Desclaux, *At. Data Nucl. Data Tables* **12**, 311 (1973).
- ²²N. Christensen, *J. Phys. F* **8**, L51 (1978).
- ²³V. Stevanović, S. Lany, X. Zhang, and A. Zunger, *Phys. Rev. B* **85**, 115104 (2012).
- ²⁴J. Vidal, X. Zhang, L. Yu, J.-W. Luo, and A. Zunger, *Phys. Rev. B* **84**, 041109 (2011).

- ²⁵X. Gonze *et al.*, *Z. Kristallogr.* **220**, 558 (2005).
- ²⁶S. Chadov, X. Qi, J. Kübler, G. Fecher, C. Felser, and S. Zhang, *Nat. Mater.* **9**, 541 (2010).
- ²⁷H. Lin, L. Wray, Y. Xia, S. Xu, S. Jia, R. Cava, A. Bansil, and M. Hasan, *Nat. Mater.* **9**, 546 (2010).
- ²⁸D. Xiao, Y. Yao, W. Feng, J. Wen, W. Zhu, X.-Q. Chen, G. M. Stocks, and Z. Zhang, *Phys. Rev. Lett.* **105**, 096404 (2010).
- ²⁹W. Feng, D. Xiao, Y. Zhang, and Y. Yao, *Phys. Rev. B* **82**, 235121 (2010).
- ³⁰R. Juza and F. Hund, *Z. Anorg. Chem.* **257**, 1 (1948).
- ³¹H. Nowotny and K. Bachmayer, *Monatsh. Chem.* **81**, 669 (1950).
- ³²A. E. Carlsson, A. Zunger, and D. M. Wood, *Phys. Rev. B* **32**, 1386 (1985).
- ³³S.-H. Wei and A. Zunger, *Phys. Rev. Lett.* **56**, 528 (1986).
- ³⁴T. Gruhn, *Phys. Rev. B* **82**, 125210 (2010).
- ³⁵Considering a hydrogenlike model for spin-orbit splitting and for a given *Z* and principal quantum number *n*, SO splitting originating from *d* orbitals is only 40% of the magnitude of SO splitting originating from *p* orbitals.
- ³⁶L. Pauling, *Phys. Rev.* **54**, 899 (1938).
- ³⁷The α type is the lowest-energy type of all the hypothetical FTS presented in this section.
- ³⁸The use of the GW-based method is then crucial in determining the correct position of the direct and indirect band gap as shown in Ref. 42.
- ³⁹C. Liu, Y. Lee, T. Kondo, E. D. Mun, M. Caudle, B. N. Harmon, S. L. Bud'ko, P. C. Canfield, and A. Kaminski, *Phys. Rev. B* **83**, 205133 (2011).
- ⁴⁰S. Chen, X. G. Gong, C.-G. Duan, Z.-Q. Zhu, J.-H. Chu, A. Walsh, Y.-G. Yao, J. Ma, and S.-H. Wei, *Phys. Rev. B* **83**, 245202 (2011).
- ⁴¹Such small crystal-field splitting is directly related to the small deviation of the kesterite structure to the zinc-blende one: $\eta = 1.017$ and $u = 0.246$.
- ⁴²J. Vidal, F. Trani, F. Bruneval, M. A. L. Marques, and S. Botti, *Phys. Rev. Lett.* **104**, 136401 (2010).